Surface Permeabilities

DOI: 10.1002/anie.200804785

Assessing Surface Permeabilities from Transient Guest Profiles in Nanoporous Host Materials**

*Despina Tzoulaki, Lars Heinke, Hyuna Lim, Jing Li, David Olson, Jürgen Caro, Rajamani Krishna, Christian Chmelik, and Jörg Kärger**

The rate of mass exchange with the surroundings is essential for the technological performance of nanoporous materials[1–3] and depends on both the diffusion coefficients within the porous material and the surface permeabilities.[4] While diffusion within porous materials has been in the focus of numerous publications,[5–8] to date the surface permeability, which is important in nanotechnology and in life sciences[9] and medicine,[10] has not been considered quantitatively. With the introduction of interference microscopy,[8,11] this deficiency may now be overcome. To date, the observation of transient concentration profiles in most of the nanoporous materials revealed substantial deviations from their ideal behavior.[12,13] Moreover, repeating adsorption–desorption cycles often lead to dramatic changes in the observed concentration patterns.[14] Only very recently, crystals of the metal–organic framework (MOF) Zn(tbip)[15] (H_2tbip = 5-*tert*-butyl isophthalic acid) proved to be stable enough to allow the essentially unlimited repetition of adsorption–desorption runs with complete reproducibility. This extraordinary quality allowed the measurement of surface permeabilities under variation of guest sizes, guest concentrations, and the type of experiment (equilibrium and non-equilibrium). Agreement between the concentration dependence of the surface permeabilities and the diffusion coefficients provides first insight into the nature of the surface resistances of these systems.

[*] D. Tzoulaki, L. Heinke, Dr. C. Chmelik, Prof. Dr. J. Kärger
Department of Experimental Physics I, University of Leipzig
Linnestrasse 5, 04103, Leipzig (Germany)
Fax: (+49) 341-973-2549
E-mail: kaerger@physik.uni-leipzig.de
H. Lim, Prof. Dr. J. Li, Prof. Dr. D. Olson
Department of Chemistry and Chemical Biology, Rutgers University
610 Taylor Road, Piscataway, NJ 08854 (USA)
Prof. Dr. J. Caro
Department of Physical Chemistry and Electrochemistry
Leibniz University of Hanover
Callinstrasse 3a, 30167 Hanover (Germany)
Prof. Dr. R. Krishna
Van't Hoff Institute for Molecular Sciences
University of Amsterdam, Nieuwe Achtergracht 166
1018 WV Amsterdam (The Netherlands)

[**] We thank German Research Foundation (DFG), INDENS Marie Curie Program, Studienstiftung des deutschen Volkes, Department of Energy (DOE) (Grant No. DE-FG02-08ER46491) for the financial support. Dr. J. M. van Baten is acknowledged for providing the snapshots of the channels.

Supporting information for this article is available on the WWW under http://dx.doi.org/10.1002/anie.200804785.

Molecular exchange between the host system and the surrounding space is described by Fick's 2nd law implemented with a boundary condition [Eqs. (1)and (2)]. D, $j(x=0)$, α, and c_{eq} denote the diffusion coefficient in the host system, flux through the surface, surface permeability, and guest concentration in equilibrium with the external atmosphere, respectively.

$$\frac{\partial c(x,t)}{\partial t} = \frac{\partial}{\partial x} D \frac{\partial c(x,t)}{\partial x} \tag{1}$$

$$j(x=0) = D\frac{\partial c(x,t)}{\partial x}\bigg|_{x=0} = \alpha(c(x=0) - c_{eq}) \tag{2}$$

Following Equation (1), the diffusion coefficient may be determined from the spatial–temporal dependence of the concentration profile.[8,11] Surface permeabilities, however, are directly accessible only at the crystal surface and, generally, have been determined by the best fit to the experimental data.[11,16] While diffusion coefficients depend on the guest concentration, surface permeation is correlated with a whole range of concentrations, from the actual boundary concentration ($c(x=0) = c_{surf}$) to the equilibrium concentration c_{eq}. We have explored the surface permeability as a function of these two limiting concentrations. Since surface permeabilities are expected to vary between different crystals, their concentration dependence must be determined with one crystal. Measurements of this type require a high degree of reproducibility which was feasible in the case of Zn(tbip).[15]

Zn(tbip) crystals have an elongated, hexagonally prismatic form with lengths of hundreds micrometers and diameters of tens of micrometers and are traversed by one-dimensional pores (Figure 1 a) along their long axis. Their synthesis is described in Ref. [15] and Figure 1 b,c show typical crystals. Samples were activated for 1.5 h under evacuation at 393 K. We selected ethane, propane, and *n*-butane as guest molecules. Sorption was initiated by varying the gas pressure in the surrounding atmosphere. The time constants of equilibration in the crystal were between 8.5–12 min for ethane and 30 h for *n*-butane. After equilibration with the surrounding gas phase, tracer-exchange experiments were started by replacing the molecules in the gas phase by their isotopes. All measurements were performed at room temperature. Concentration profiles were recorded by interference microscopy[8,11,16] and IR micro-imaging[17] (see the Supporting Information for details).

Figure 2 shows the permeability data obtained for one crystal from a large number of adsorption and desorption

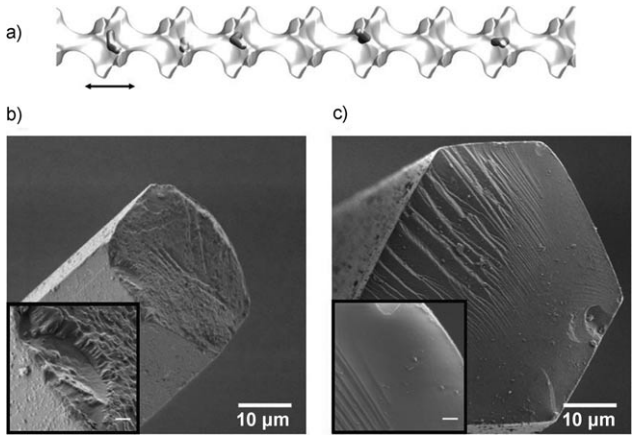

Figure 1. a) Schematic representation of a one-dimensional channel (segment indicated by arrow) along the long axis of a Zn(tbip) crystal with propane guest molecules. SEM images of the face surface b) of an as-synthesized crystal and c) of a freshly cut crystal. Insets: enlargements (scale bars: 1 μm).

runs. The concentration profiles provide both the boundary concentrations and surface fluxes which, on the basis of Equation (2), are used to determine the surface permeability for each value of c_{surf}. These permeabilities are indicated in Figure 2 as blue dots.

Importantly, the permeability data for a pair of values c_{eq} and c_{surf} are independent of the sorbate concentration in the crystal at the beginning of the experiment. This is exemplified by two experiments with an equilibrium concentration of $c_{eq} = 0.9$ and boundary concentrations $c_{surf} = 0$ to 0.9 (Figure 2, open circles) and from 0.5 to 0.9 (Figure 2, filled circles), from experiments with two different pressure steps. Since the permeabilities are expected to exclusively depend on the boundary and equilibrium concentrations (and to remain unaffected, therefore, by the concentration profiles within the crystallite which differ for different pressure steps), this agreement confirms the self-consistency of our measurements.

Since dependence on two separate parameters would dramatically impede the practical use of surface permeabilities we looked for some way of combining these parameters. Surface permeability was found to be reasonably well represented as a function of the arithmetic average of the equilibrium and boundary concentrations $(c_{eq} + c_{surf})/2$. The result of a corresponding fitting procedure is indicated in Figure 2 by the three-dimensional surface with colors varying from black to red for permeabilities increasing from about 1.2 to $5.5 \times 10^{-8}\ m\,s^{-1}$. The surface permeability is thus found to be essentially independent of the difference between the actual and the equilibrium surface concentration, that is, of the height of the pressure step, and symmetric with respect to adsorption and desorption.

Figure 3a shows the surface permeability data of Figure 2 as a function of $(c_{eq} + c_{surf})/2$ as well as the transport diffusion coefficients of propane calculated form the transient concentration profiles using Equation (1). Comparison of the concentration dependencies reveals a remarkable similarity. This

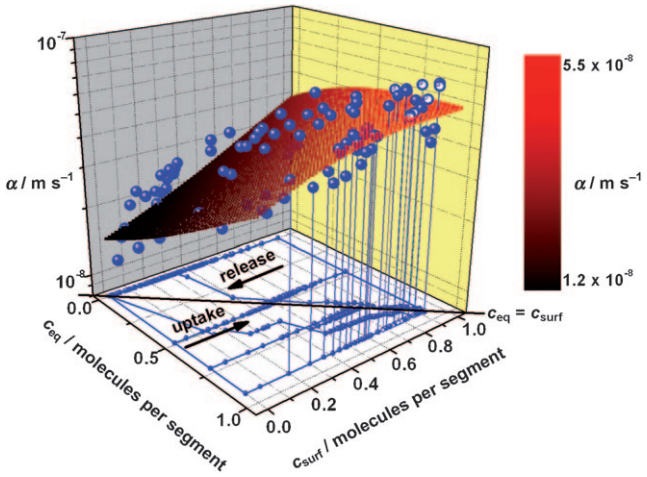

Figure 2. Surface permeability α of propane (blue dots) as a function of the equilibrium concentration c_{eq} and the surface concentration c_{surf} of the crystal. The date are obtained by six uptake and six release experiments (each of 5 runs under constant pressure and 1 run under variable pressure). The projection of each blue point on the bottom plane gives the corresponding pair of the equilibrium and surface concentrations, provided by the respective transient profiles monitored by interference microscopy. Every straight line along the axis of the surface concentration with constant equilibrium concentration belongs to an adsorption ($c_{surf} < c_{eq}$) or desorption ($c_{surf} > c_{eq}$) experiment under constant pressure. The two curves belong to adsorption–desorption cycles under variable pressure. The inserted surface represents the best fit of the surface permeability as a function of the average concentration ($(c_{eq} + c_{surf})/2$). The open blue symbols belong to an experiment with initial concentration of 0.5 to an equilibrium concentration of 0.9 molecules per segment.

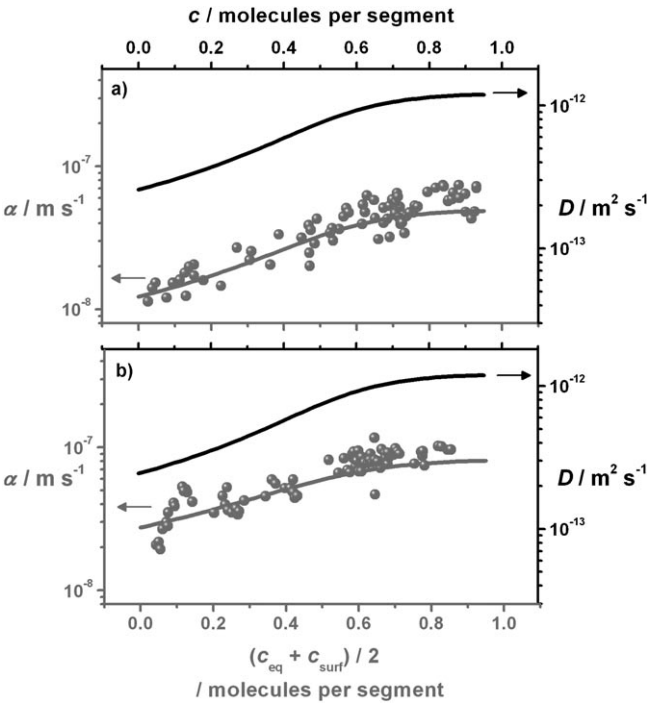

Figure 3. Transport diffusion coefficient D (top line) and surface permeability α (dots/lower line) of propane a) in the Zn(tbip) crystal considered in Figure 2 and b) in another as-synthesized crystal from the same sample, as a function of the (mean) concentration $((c_{eq} + c_{surf})/2)$.

agreement was also found for a second crystal from the same sample (Figure 3b) which indicates this behavior to be a general trend. Note that the diffusion coefficients measured for different specimens form the same sample are found to vary by less than 20%, whereas the surface permeabilities may differ by factors of up to 2. This finding corresponds to the fact that, on comparing different crystallites, the pore space remains essentially the same while surface properties, including the permeabilities, can vary much more readily between different specimens.

Figure 4a and b shows the diffusion coefficients and surface permeabilities for the guests ethane and *n*-butane. For *n*-butane, both the diffusion coefficients and the permeabilities follow the concentration dependence observed with propane, but at slightly smaller values. Given the coinciding kinetic diameter (ca. 4.3 Å)[18] and the slightly longer length of butane, this is the expected behavior. The dramatic increase in surface permeability (by two orders of magnitude) and diffusion coefficient for ethane molecules, as well as the differences in the concentration dependence, may be associated with ethane's much smaller kinetic diameter of approximately 3.8 Å.[18] Figure 4c shows the propane (transport) diffusion coefficients and surface permeabilities (data as in Figure 3a) obtained in transient sorption experiments, that is, under non-equilibrium conditions, and the results of isotope exchange, that is, the corresponding equilibrium data from IR micro-imaging. The self-diffusion coefficients are found to be notably smaller than the transport diffusion coefficients and to decrease rather than to increase with increasing loading. Both differences may be correlated with the steric properties of the pore space. It consists of segments (see Figure 1a) which, in general, cannot accommodate more than one guest molecule. Therefore, exchange between adjacent molecules in a pore chain is greatly impeded. While transport diffusion is unaffected by the mutual exchange of adjacent molecules and, thus not influenced by its impedance, such exchange is the governing process of tracer-exchange experiments and, thus, of self-diffusion. Self-diffusion coefficients, therefore, must be significantly smaller than the transport diffusion coefficients, and decrease with increasing loading. In tracer-exchange experiments, the surface permeabilities are found to have a similar concentration dependence to the diffusion coefficients, that is, they decrease with increasing loading.

This remarkable correlation between diffusion coefficients and surface permeation suggests that the transport resistance exerted by the crystal surface is brought about by total blockage of a certain (large) fraction of the pore openings rather than by a partial obstruction of all of them. In accordance, Figure 1b shows a partial overgrowth which could be the structural origin of the surface resistance. Imperfections in the interior of the crystal structure allow equilibration of the guest concentration over the whole pore array.

The stochastic nature of the surface resistances and differences in the overgrowth lead to a variation in their intensity for different crystals. These differences are notably larger than the scattering of the values for one and the same crystal, which is caused by the small, but inevitable uncertainty of the recorded concentrations (see Supporting Information).

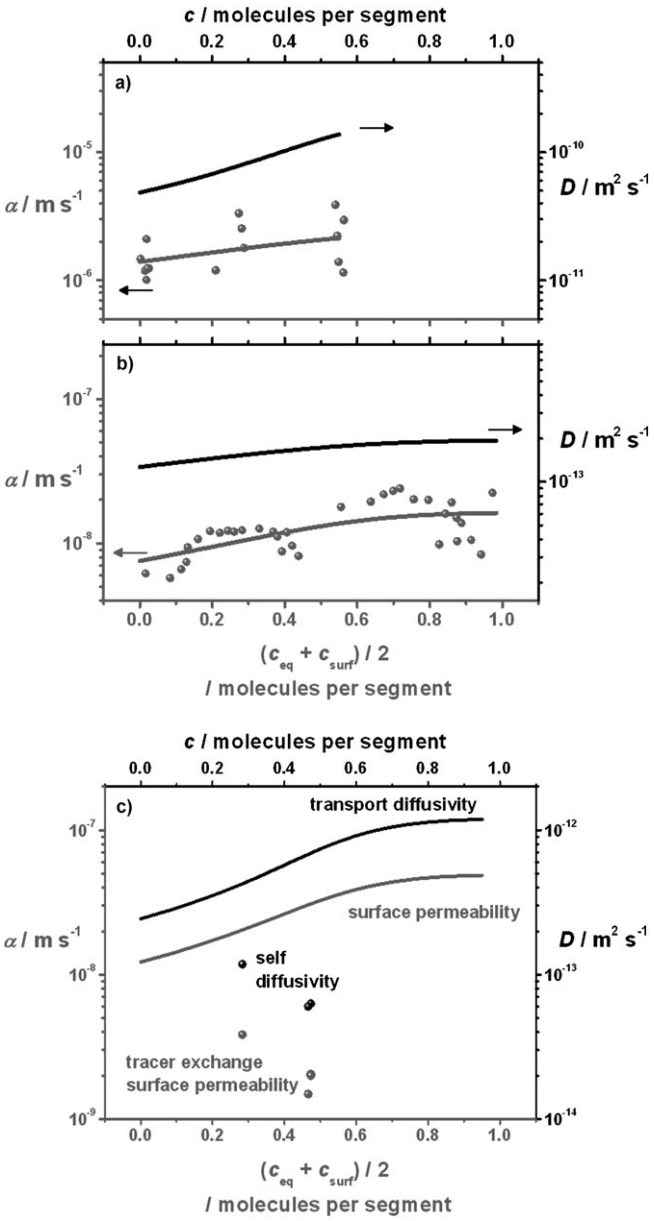

Figure 4. Diffusion coefficients *D* and surface permeabilities α for transient sorption experiments at room temperature with a) ethane and b) *n*-butane on the same crystal as considered in Figure 3b. c) Comparison of the propane data for transient sorption with the corresponding data under equilibrium conditions (self-diffusion coefficients and tracer-exchange surface permeabilities).

In our experiments we observed that the surface permeabilities on either side of a given crystal are similar. This result indicates that the crystallization process itself does not give rise to the formation of surface barriers, since then it would be difficult to explain why the surface permeabilities differ from crystal to crystal but are the same on either side of a given crystal. The formation of surface resistances should rather be associated with the influence of the crystal surroundings which, during crystallization and crystal storage until per-

forming the experiments, should be more similar on either side of the same crystal than for different ones.

This symmetry is expected to be revoked by creating surfaces with different "histories" on either side of the same crystal. For this purpose we have broken a crystal just before the sorption experiment within the observation cell (see Figure SI4 in the Supporting Information). As expected, the permeability at the fractured surface (Figure 1c) is approximately 10 times larger than on the other (the "old") surface (Figure 1b).

A detailed data set for the quantification of surface permeabilities was established. The remarkable concurrence with the diffusion coefficients indicates a close relationship between the elementary processes of diffusion and permeation, suggesting that permeation proceeds through relatively small surface areas of essentially infinitely high permeability, and that over the vast majority of the surface the pore entrances are blocked. The surface resistances observed with the first uptake after activation were reproduced with all subsequent release and uptake experiments. Hence, in contrast to the experiments reported in Ref. [14], in which, with increasing number of adsorption–desorption cycles, the uptake of isobutane in silicalite-type crystals was found to be progressively retarded by the formation and intensification of surface barriers owing to spurious water in the guest atmosphere, the adsorption–desorption cycle itself does not contribute to the formation of the observed surface barrier. Based on the evidence of the microscope images (Figure 1b and c) it may be assumed that amorphous layers, partially covering the crystal surface, give rise to the observed surface resistances. In addition, the surface resistances may be caused by bulky molecules absorbed close to the surface layer which cannot be removed by a simple evacuation procedure between the individual adsorption–desorption runs. Removal of such contaminations would require high-temperature treatment which, presently, is not possible under the microscope. Thus, further experimental refinement with the option to identify a particular crystallite even after high-temperature treatment is among the crucial prerequisites for completing our present view on the formation of surface barriers. These efforts will be promoted by the technological interest in these materials and by the relevance of transport phenomena in their application.

Received: October 1, 2008
Revised: December 10, 2008
Published online: April 3, 2009

Keywords: coordination polymers · nanoporous materials · surface permeability · surface resistance

[1] F. Schüth, K. S. W. Sing, J. Weitkamp, *Handbook of Porous Solids*, Wiley-VCH, Weinheim, **2001**.
[2] G. Ertl, H. Knözinger, F. Schüth, J. Weitkamp, *Handbook of Heterogeneous Catalysis*, Wiley-VCH, Weinheim, **2008**.
[3] M. Dincă, J. R. Long, *Angew. Chem.* **2008**, *120*, 6870; *Angew. Chem. Int. Ed.* **2008**, *47*, 6766.
[4] J. Crank, *The Mathematics of Diffusion*, Clarendon, Oxford, **1975**.
[5] "Diffusion in zeolite molecular sieves": D. M. Ruthven, M. F. M. Post in *Introduction to Zeolite Science and Practice*, Elsevier, Amsterdam, **2001**.
[6] J. Kirstein, B. Platschek, C. Jung, R. Brown, T. Bein, C. Bräuchle, *Nat. Mater.* **2007**, *6*, 303.
[7] R. Krishna, J. M. van Baten, *Microporous Mesoporous Mater.* **2008**, *109*, 91.
[8] D. Tzoulaki, L. Heinke, W. Schmidt, U. Wilczok, J. Kärger, *Angew. Chem.* **2008**, *120*, 4018; *Angew. Chem. Int. Ed.* **2008**, *47*, 3954.
[9] R. Bausinger, K. von Gersdorff, K. Braeckmans, M. Ogris, E. Wagner, C. Bräuchle, A. Zumbusch, *Angew. Chem.* **2006**, *118*, 1598; *Angew. Chem. Int. Ed.* **2006**, *45*, 1568.
[10] C. Xiao, D. J. Moore, M. E. Rerek, C. R. Flach, R. Mendelsohn, *J. Invest. Dermatol.* **2005**, *124*, 622.
[11] J. Kärger, P. Kortunov, S. Vasenkov, L. Heinke, D. B. Shah, R. A. Rakoczy, Y. Traa, J. Weitkamp, *Angew. Chem.* **2006**, *118*, 8010; *Angew. Chem. Int. Ed.* **2006**, *45*, 7846.
[12] E. Lehmann, S. Vasenkov, J. Kärger, G. Zadrozna, J. Kornatowski, Ö. Weiss, F. Schüth, *J. Phys. Chem. B* **2003**, *107*, 4685.
[13] E. Lehmann, C. Chmelik, H. Scheidt, S. Vasenkov, B. Staudte, J. Kärger, F. Kremer, G. Zadrozna, J. Kornatowski, *J. Am. Chem. Soc.* **2002**, *124*, 8690.
[14] D. Tzoulaki, W. Schmidt, U. Wilczok, J. Kärger, *Microporous Mesoporous Mater.* **2008**, *110*, 72.
[15] L. Pan, B. Parker, X. Huang, D. H. Olson, J. Y. Lee, J. Li, *J. Am. Chem. Soc.* **2006**, *128*, 4180.
[16] P. Kortunov, L. Heinke, S. Vasenkov, C. Chmelik, D. B. Shah, J. Kärger, R. A. Rakoczy, Y. Traa, J. Weitkamp, *J. Phys. Chem. B* **2006**, *110*, 23821.
[17] C. Chmelik, A. Varma, L. Heinke, D. B. Shah, J. Kärger, F. Kremer, U. Wilczok, W. Schmidt, *Chem. Mater.* **2007**, *19*, 6012.
[18] D. W. Breck, *Zeolite Molecular Sieves*, Wiley, New York, **1974**.

Angewandte Chemie
Eine Zeitschrift der Gesellschaft Deutscher Chemiker

Supporting Information

69451 Weinheim, Germany

Assessing surface permeabilities from transient guest profiles in nanoporous host materials

*Despina Tzoulaki, Lars Heinke, Hyuna Lim, Jing Li, David Olson, Jürgen Caro, Rajamani Krishna, Christian Chmelik and Jörg Kärger**

1 Methods

1.1 Interference Microscopy

A Jenamap p dyn (Carl Zeiss GmbH) interference microscope equipped with an interferometer of the Mach-Zehnder type is the basic technique used for the purpose of this study. Its high spatial resolution (0.5 × 0.5 μm^2) together with the time resolution (10 s) enabled us to record with high accuracy the transient concentration profiles of the guest molecules. On the basis of this technique, we correlate the optical path length of the beam passing through the crystal under study with the refractive index of the medium (crystal) and with the actual intracrystalline concentration. The first quantity is measured, the latter is determined (see Fig. SI1). A fully detailed description of the method can be found in refs. 1 and 2.

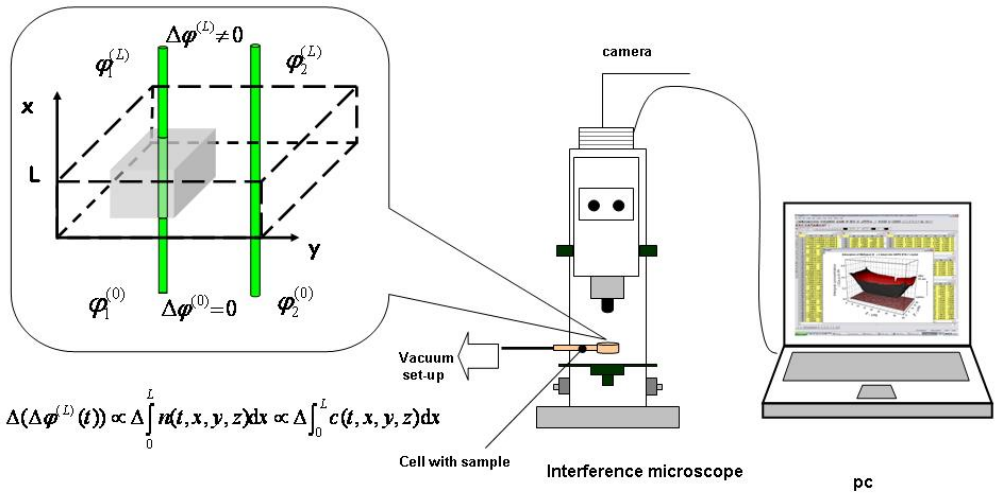

Fig. SI1: Schematical representation of the principle of IFM (left), of the microscope (middle) and of the pc for the treatment of the raw data (right).

1.2 IR Microscopy

In addition, transient concentration profiles were recorded using a HYPERION 3000 IR microscope (Bruker), equipped with a 128 × 128 IR imaging detector.[3] The concentration profiles in individual crystals were obtained by following the intensity of characteristic absorption bands. The integrals under these bands were assumed to be proportional to the integrals of the local concentration in the direction of the IR beam (see Fig. SI2). The ability to pinpoint adsorbates by their characteristic IR bands allows tracer self-exchange measurements, from which the self-diffusivity and tracer exchange surface permeability can be calculated.

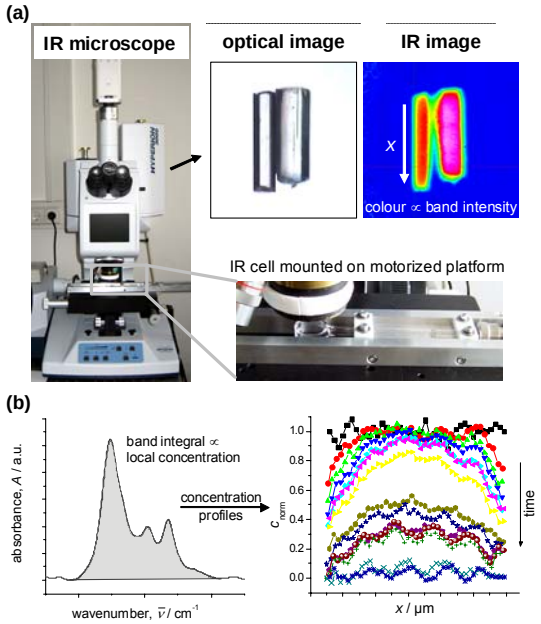

Fig. SI2: a) Photograph of the Infra-Red microscopy (IRM) experimental set-up. The two upper-right pictures show the MOF crystals recorded with the microscope operated in the viewing mode and IR mode, respectively. For each IR pixel the full spectral information is recorded, although the IR image shows the intensity of one selected band only. b) The absorbance spectra of all IR pixels are integrated at one selected IR band to obtain the local concentration of the guest molecule. The concentration measured for different times is plotted over the crystal extension along *x* (direction of channels) to obtain the transient concentration profiles.

2 Transient Concentration Profiles

2.1 Profiles determined by interference microscopy

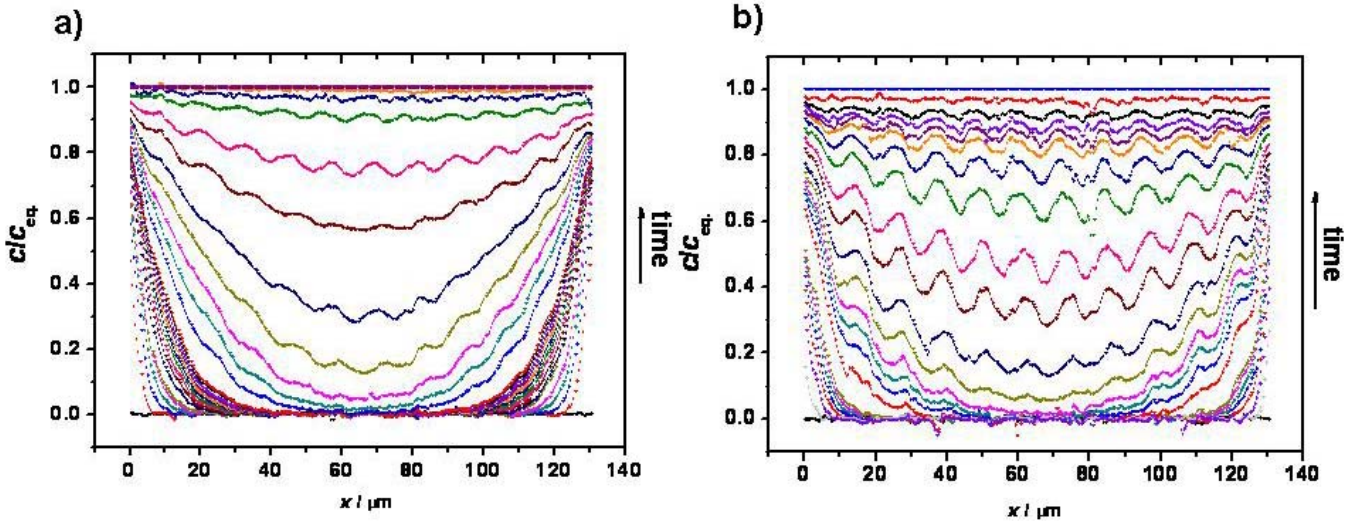

Fig. SI3: Evolution of transient concentration profiles in the case of propane a) 0→0.93 molecules per segment and b) 0→0.32 molecules per segment, as recorded by interference microscopy.

2.2 Profiles determined by IR micro-imaging

The results obtained by interference microscopy were complemented by measurements using IR micro-imaging. The main focus was given to tracer-exchange experiments, where the self-exchange of propane with its fully deuterated isotope was monitored. Two representing cases are shown in Fig. SI4. The experiments are initiated by replacing the gas phase surrounding the crystal with the corresponding isotope.

Since the exchange proceeds under equilibrium conditions, (tracer-)self- diffusivity and tracer exchange surface permeability can be obtained from such data.

To support the hypothesis that the observed surface barrier is related with amorphous layers partially covering the crystal surface (Fig. 1b of main paper), crystals were cut at one edge. The face surfaces of freshly cut crystals were found to be much smoother and show no indications for any overgrowth (Fig. 1c of main paper). Following our hypothesis, one should expect that cutting crystal edges reduces the surface barrier drastically. The concentration profiles recorded for such crystals were indeed highly asymmetric (Fig. SI4b) as expected if the two crystal faces exhibit notably different surface permeabilities. The analysis of these profiles showed that the permeability of freshly cut faces could be increased by about one order of magnitude compared to the other, as synthesized, "reference face" of the crystal.

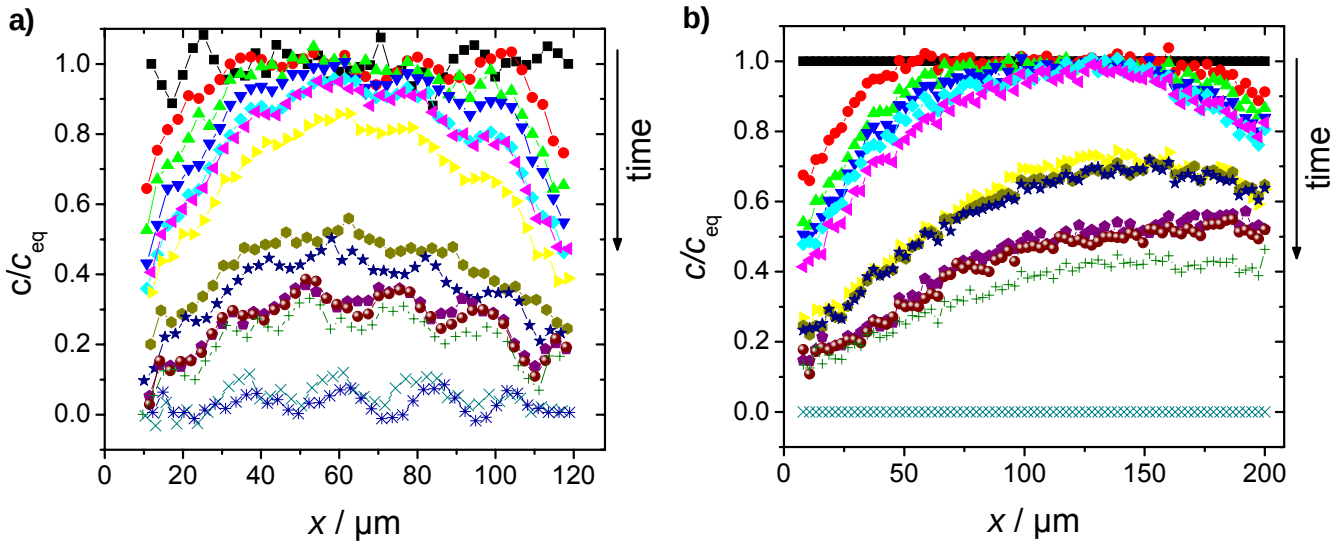

Fig. SI4: Evolution of transient concentration profiles during tracer exchange of propane (desorbing isotope) for the loadings a) 0.48 molecules per segment and b) 0.29 molecules per segment, as recorded by IR micro-imaging. b) The profiles for crystals with one freshly cut edge (left end) are highly asymmetric. By cutting, the permeability could be increased by one order of magnitude compared to the as-synthesized face.

3 Determining the transport parameter

The surface permeability α is calculated directly by determining the flux through the surface and rearranging equation (2). Moreover, the transport parameters are determined by fitting the measured concentration profiles with a numerical solution of Fick's 2nd law.[4,5] The quasi-chemical approach of Reed and Ehrlich[6-8] was applied to find one set of transport parameters which is able to describe all profiles obtained for one kind of guest molecule.

The recorded concentrations have a small, but inevitable uncertainty. Furthermore, the concentration profiles are superimposed by small oscillations which are associated with partial reflection at the interfaces crystal–gas causing constructive and destructive interference (see Fig SI 3 and ref. 9). These data imperfections impair the accuracy of the determined fluxes and boundary concentration leading to the scattering of the calculated surface permeabilities. The relative standard deviation of the surface permeability according to the best fit by means of the Reed-Ehrlich model results in 33 %. It is noteworthy that the results have neither been averaged nor smoothed.

[1] U. Schemmert, J. Kärger, J. Weitkamp, *Microporous Mesoporous Mater.* **1999**, *32*, 101.
[2] J. Kärger, P. Kortunov, S. Vasenkov, L. Heinke, D. B. Shah, R. A. Rakoczy, Y. Traa, J. Weitkamp, *Angew. Chem. Int. Ed.* **2006**, *45*, 7846.
[3] L. Heinke, C. Chmelik, P. Kortunov, D. M. Ruthven, D. B. Shah, S. Vasenkov, J. Kärger, *Chem. Eng. Technol.* **2007**, *30*, 995.
[4] J. Crank, *The Mathematics of Diffusion*, Clarendon Press, Oxford, **1975**.
[5] L. Heinke, J. Kärger, *New Journal of Physics* **2008**, *10*, 023035.
[6] D. A. Reed, G. Ehrlich, *Surf. Sci.* **1981**, *102*, 588.
[7] R. Krishna, D. Paschek, R. Baur, *Microporous Mesoporous Mater.* **2004**, *76*, 233.
[8] G. K. Papadopoulos, H. Jobic, D. N. Theodorou, *J. Phys. Chem. B* **2004**, *108*, 12748.
[9] T. L. Schmitz, A. Davies, C. J. Evans, R. E. Parks, *Optical Eng.* **2003**, *42*, 2281.